Mat. Res. Soc. Symp. Proc. Vol. 674 © 2001 Materials Research Society

Effects of Substrates on the Self-Assembling of FePt Nanocrystals

Min Chen and David E. Nikles*
The University of Alabama, Tuscaloosa,
Center for Materials for Information Technology,
Box 870209, Tuscaloosa, Alabama, 35487-0209, US
*dnikles@mint.ua.edu

ABSTRACT

$Fe_{48}Pt_{52}$ nanoparticles were synthesized by the simultaneous chemical reduction of platinum acetylacetonate and thermal decomposition of iron pentacarbonyl. As-prepared the particles were spherical with an average diameter of 3 nm and a polydispersity of less than 5%. The particles were superparamagnetic and had a fcc structure. Highly ordered self-assembled supercrystals of particles were formed in TEM grids by deposition from dispersions in hydrocarbon solvents. Nanoparticles deposited on amorphous carbon-coated and SiO_2-coated Cu grids tend to assemble into small domains of hexagonal arrays. Larger domains of hexagonal arrays formed on Si_3N_4 membrane TEM grids. For thin multilayers, the FePt nanoparticles tends to assemble into hexagonal close-packed lattices (ABABAB stacking). For the thicker multilayers, ABCABC stacking was observed. Small angle X-ray reflectivity of the particles on a Si (100) substrate show highly ordered multiplanar structure with d-spacing of 6.2 nm. The coercivity of self-assembled FePt films strongly depended on the annealing temperature. After annealing at 700°C for 30 minutes, the particles transformed from FCC to "FCT" phase and the coercivity of film increased up to 11570 Oe. However, the particle size increased to 16 nm due to sintering.

INTRODUCTION

The "face-centered tetragonal" phase FePt is emerging as an important material in ultrahigh density magnetic data storage media. This phase has large uniaxial magnetocrystalline anisotropies (K_u) due to its tetragonal structure. The study of nanoscale magnetic domains are of both fundamental and pressing technical interest. The grain size of advanced recording media is rapidly being reduced to dimensions, where the magnetic materials approach the superparamagnetic limit. Development of a detailed understanding of the properties of magnetic nanocrystals is essential to the development of future magnetic recording technology. It is expected that if an ordered monolayer is formed by magnetic nanocrystals with sizes down to ~3 nm, the storage density can be up to 100-1000 Gbits/in^2 [1-2].

There are three conventional methods for magnetic material processing: vacuum sputtering, physical vacuum evaporation and molecular bean epitaxy. Chemical vacuum evaporation and electrochemical deposition are also used in processing the magnetic thin film. Progress in magnetic recording density is due in part to the development of media with finer and finer grain magnetic films [3-9].

Processing of ordered 2D or 3D structure of magnetic nanocrystalls becomes an area of great interest for the thin granular films. The synthesis of nanoparticles, characterized by a narrow size distribution, is a new challenge in solid-state chemistry. Due to their small size, nanoparticles exhibit novel material properties that differ considerably from those of the bulk

solid state. Up to date, ordered self-assembly of nanocrystals has been successfully fabricated for several materials, such as Ag [10], Au [11], Fe_2O_3 [12], CoO [13]. Recently, two chemical methods have been employed to produce magnetic cobalt nanoparticles, including solution phase metal salt reduction in reverse micelles [14] or in an organic solvent [15]. Ordered arrays of nanocrystal FePt alloy have also been reported [16], demonstrating the possibility of self-assembly of magnetic nanoparticles.

In the present paper, we try to understand the effect of substrates and other factors on self-assembly of FePt nanoparticles.

EXPERIMENTAL DETAILS

Materials and sample preparation

All materials were used without further purification. $Fe(CO)_5$, platinum acetylacetonate, octyl ether, oleic acid and oleylamine were purchased from Aldrich. Hexane and octane were purchased from Fisher Scientific.

FePt nanocrystals were processed by simultaneous thermal decomposition of $Fe(CO)_5$ and reduction of platinum acetylacetonate, $Pt(acac)_2$, in octyl ether, following Sun's procedure [16]. The particles were dispersed in a 50/50 mixture of hexane and octane, then dropped onto carbon-coated TEM grids, SiO_2 coated TEM grids or Si_3N_4 membrane window TEM grids. The solvent was allowed to evaporate. Samples were annealed under vacuum ($<1 \times 10^{-7}$ torr) at 500°C, 600°C or 700°C for 30 minutes. Samples assembled and annealed on SiO_2/Si(100) wafer were also prepared for EDS, XPS, X-ray diffraction & scattering, and magnetic measurements.

Characterization

Wide angle X-ray diffraction (XRD) data were acquired on Rigaku D/MAX-2BX Horizontal XRD Thin Film Diffractometer. The small angle X-ray scattering (SAXS) data from 0.2 to 5° (2θ) were collected on Philips X'Pert system X-ray diffractometer using Cu Kα radiation and by activating beam attenuator Ni 0.125 mm (factor 151.00). A graded parabolic focusing mirror was utilized to transform a divergent X-ray beam into a quasi-parallel yet intensive incident beam with angular divergence of about 0.05°. Transmission electron microscopy (TEM) microphotographs were carried out on a Hitachi 8000 electron microscope operating at 200 kV. Energy disperse spectroscopy (EDS) were obtained with a Philips model XL 30 scanning electron microscope equipped with EDS. Chemical analysis was carried out with Kratos Axis 165 XPS/Auger system. Magnetic measurement was obtained with Princeton Micromag™ 2900 alternating gradient magnetometor (AGM).

RESULTS AND DISCUSSIONS

Ordered self-assembling of as-prepared FePt nanocrystals

Figure 1 (a-d) shows the ordered monolayer of FePt nanoparticles on different kinds of TEM grids. The size distribution of FePt nanoparticleswere determined from the TEM image. The average diameter was 3 nm with a polydispersity of <5%. Magnetic measurement shows that these FePt nanoparticles were superparamagnetic. In general, FePt nanoparticles tended to self-

assemble into hexagonal monolayers. We found mutiple hexagonal domains of FePt particles on carbon-coated TEM grids and on SiO_2-coated TEM grids. On Si_3N_4 membrane grids the hexagonal domains were much larger, on the order of 800 nm. The nearest neighbor particle distance is in the range of 7.4-8.0 nm. The small angle electron diffraction in the insert of Fig. 1b shows a hexagonal ring. This also indicated the forming of various small domains of hexagonal arrays in different orientations. The small angle electron diffraction in the insert of Fig. 1c show hexagonal-spot pattern. The nearest neighbor particle distance is 7.6 nm. Interestingly, when the concentration of FePt is too low to form a continuous monolayer on Si_3N_4 membrane TEM grids, FePt nanoparticles still form discontinuous hexagonal arrays but in almost the same direction, as shown in Fig.1d. The carbon and SiO_2 coatings on TEM Cu grids are amorphous, while Si_3N_4 membrane is believed to be single crystal. The above evidence suggests the effect of substrates on the forming first layer self-assembling of nanoparticles.

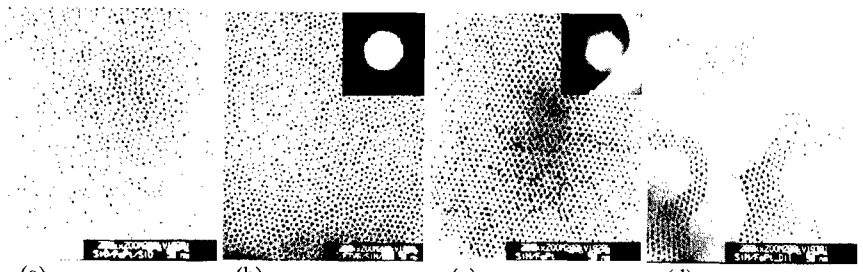

(a) (b) (c) (d)

Figure 1. TEM images of ordered 2-D FePt on (a) SiO_2-coated Cu grid, (b) carbon-coated Cu grid, and (c) & (d) Si_3N_4 membrane TEM grids. The inserts in (b) and (d) are small angle electron diffraction patterns of samples.

For the multilayer FePt nanoparticles on different kinds of TEM grids, the TEM pictures show that "honeycomb" arrays of FePt on a carbon-coated Cu TEM grid (Fig2a) and wire superlattice on a SiO_2-coated Cu TEM grid (Fig. 2b). Actually, we also found "honeycomb" arrays of FePt on SiO_2-coated Cu grids and wire arrays on carbon-coated Cu grids. They both come from the hexagonal close-packing (HCP, ABAB stacking) of FePt. The honeycomb arrays can be transformed into wire array for HCP structure if changing the viewing from the [001] to the [211] direction. The small angle electron diffraction of "honeycomb" FePt structure confirms the hexagonal stacking with lateral d-spacing of 6.56 nm, which is twice the particle size. When the thickness of multilayer films increase, FePt nanoparticles self-assemble into square array on SiO_2-coated Cu grid (Fig. 2c) and highly ordered hexagonal arrays on Si_3N_4 membrane TEM grid. The square arrays (more exactly, FCC superlatice) can be viewed as ABCABC close-packing of nanoparticles from [111] direction.

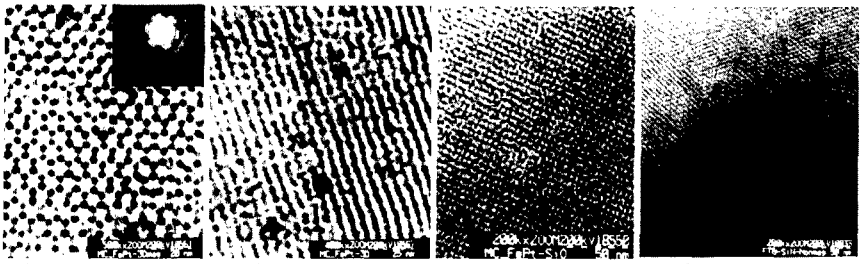

(a) (b) (c) (d)

Figure 2. TEM images of ordered 3-D FePt on (a) carbon-coated Cu grid, (b)&(d) SiO_2-coated Cu grid, and (d) Si_3N_4 membrane TEM. The insert in (a) is small angle electron diffraction pattern of sample.

Small angle X-ray scattering (Fig.3) reveals the highly ordered multiplayer structure of FePt/surfactants with periodic thickness of 6.2 nm while as-depositing on SiO_2/Si(100) wafer. The periodic thickness is also the d-spacing of nearest neighbor FePt layers [17]. Similar to Ref.[18], the analysis of peak positions show the FePt is likely to be HCP superlattice .

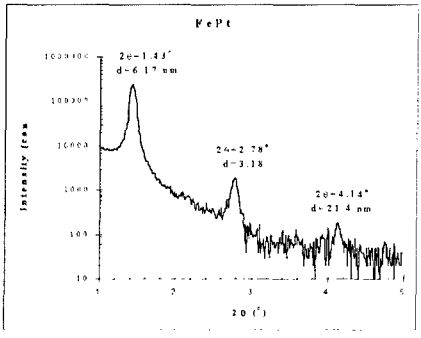

Figure 3. SAXS of ordered FePt multilayer on SiO_2/Si(100) waver.

Mechanism of forming ordered assembled FePt film

The ordered HCP superlattice formation has been shown to apply to a variety of materials when the nanoparticles are stabilized by surfactant [10-16]. Molecular dynamics simulations shows that, without interparticle attraction, monodispersed hard spheres order when particle concentrations exceed a critical volume fraction of 0.49 [19]. In this case, the repulsion between particles must dominate when particles approach each other. Entropy is only the driving force for disorder-order phase transitions of hard spheres. HCP or FCC arrays are formed because they are the lowest energy state of stacking. Korgel's model shows that the balance between the interparticle attraction and the attraction between particles and the substrate (which can be tuned by solvent polarity) determines film structure, especially thickness while permitting nanoparticles to self-assemble into a HCP structure [20].

The attractive capillary force might be the main factor governing the ordering. It is reported that, for micro-size latex particles, HCP superlattice start to form when the thickness of the solvent layer approach the particle diameter during evaporation [21].

Effects of Annealing Temperature on FePt

Table I shows the temperature effect on the phase transformation, sintering and magnetic properties of FePt. When the annealing temperature increase to 500°C, FePt nanoparticles began to transform from fcc to tetragonal. The order parameter, S, was determined from the ratio of the c axis to the a axis lattice parameters as measured from x-ray diffraction. Increasing the annealing temperature increased the ordering parameter and the coercivity. The grain size was determined from the linewidth of the x-ray diffraction peaks. In our hands annealing the FePt articles resulted in significant increases in grains size.

Table I. Effect of annealing temperature on the crystallite size, ordering parameter, and magnetic properties of FePt films on silicon.

Annealing Temperature (°C)	Ordering parameter, S	Grain Size (nm)	Coercivity (Oe)
500	0.22	3.0	3970
600	0.52	7.6	6500
700	0.88	16.0	< 11600*
	S=(1-(c/a))/(1-0.961)		* minor loop

XPS depth profile of FePt shows that after vacuum annealing at 600°C for 30 minutes, iron is mostly in Fe (+2) state at the surface of FePt film, and in Fe (0) state in the bulk of the film. Platinum is in the metallic Pt (0) state through all the film. Fe and Pt never react with Si to form silicided FePt film even after annealing at 700°C.

CONCLUSIONS

For monolayer deposition, the as-deposited FePt tend to assembly into small domains of hexagonal arrangements nanoparticles on amorphous carbon-coated and SiO_2-coated Cu grids, while forming larger single domain of hexagonal arrangement on Si_3N_4 membrane. For the thin multilayer, the FePt nanoparticles tends to assembly into HCP (ABABAB stacking) on TEM grids (either carbon or SiO_2-coated). For the thick multilayer, FePt tends to form ABCABC close packing on TEM grids. Small angle X-ray scattering of as-deposited FePt on Si (100) substrate show highly ordered multiplayer structure with d-spacing of 6.2 nm between layers. The coercivity of self-assembled FePt film strongly depends on the annealing temperature. After annealed at 700 °C for 30 minutes, 88% of FePt nanocrystal transform from FCC to "FCT" phase, and the coercivity of film increase up to 11570 Oe with the squareness of 0.70. However, The particle size increase to 16 nm due to sintering. Processing high coercivity FePt film without significant sintering is the priority of our future work.

ACKNOWLEDGMENTS

The authors would like to thank Drs. J. A. Barnard and J. W. Harrell for suggestions on research related to the present paper. Special thanks to Dr. E. Edar, Mr. M Sun and Mr. F. Liu for giving Min Chen assistance in running XPS, AGM and SAXS. Research supported by the NSF Materials Research Science and Engineering Center award number DMR-9809423.

REFERENCES

1. D. Weller, A. Moser, L. Folks, M. E. Best, W. Lee, M. F. Toney, M. Schwickert, J.-U. Thiele, and M. F. Doerner, *IEEE Trans. Magn.* **36**, 10 (2000)
2. J. Numazawa and H. Ohshima. *J. Magn. Magn. Mater.* **176**, 1 (1997).
3. E. S. Murdock, R. F. Simmons, and R. Davison, *IEEE Trans. Magn.* **28**, 3078 (1992).
4. T. Yogi and T. A. Nguyen, *IEEE Trans. Magn.* **29**, 307 (1993).
5. P.-L. Lu and S. H. Charap, *IEEE Trans. Magn.* **30**, 4230 (1994).
6. E. Grochowski and D. A. Thompson, *IEEE Trans. Magn.* **30**, 3797 (1994).
7. R. M. H. New, R. F. W. Pease, and R. L. White, *J. Vac. Sci. Technol.* **B12**, 3196 (1994).
8. D. N. Lambeth, E. M. T. Velu, G. H. Bellesis, L. Lee, and D. E. Laughlin, *J. Appl. Phys.* **79**, 4496 (1996).
9. S. H. Charap, P.-L. Lu, and Y. He, *IEEE Trans. Magn.* **33**, 978 (1997).
10. P.C. Ohara, J.R. Heath and W.M. Gelbart. *Angew. Chem. Int. Ed. Engl.* **36**, 1078 (1997).
11. R.P. Andres, J.D. Bielefeld, J.I. Henderson, D.B. Janes, V.R. Kolagunta, C.P. Kubiak, W.J. Mahoney and R.G. Osifchin. *Science* **273**, 1690 (1996).
12. M.D. Bentzon, J. Van Wonterghem, S. Mrup, A. Thölen and C.J.W. Koch. *Phil. Mag. B.* **60**, 169 (1989).
13. J.S. Yin and Z.L. Wang. *J. Mater. Res.* **14**, 503 (1999).
14. Taleb, A.; Petit, C.; Pileni, M. P. *Chem. Mater.* **9**, 950. (1997).
15. S. Sun and C.B. Murray. *J. Appl, Phys.* **85**, 4325 (1999).
16. S. Sun, C.B. Murray, D. Weller, L. Folks and A. Morser. *Science.* **287**, 1989 (2000).
17. A. County, C. Fermon and M.-P. Pileni. *Adv. Mater.* **13**, 254 (2001).
18. H. Zabel. *Appl. Phys.* A **58**, 159 (1994).
19. B. J. Alder; W. G. Hoover; and D. A. Young. *J. Chem. Phys.*, **49**, 3688 (1968).
20. B. A. Korgel and D. Fitzmaurice. *Phys. Rev. Lett.* **80**, 3531 (1998).
21. N. D. Denkov; O. D. Velev; P. A. Kralchevsky, I. B. Ivanov; H. Yoshimura; and K. Nagayama. *Langmuir*, **8,** 3183 (1992).